Adipose-specific disruption of autotaxin enhances nutritional fattening and reduces plasma lysophosphatidic acid

Rodolphe Dusaulcy,[*,†] Chloé Rancoule,[*,†] Sandra Grès,[*,†] Estelle Wanecq,[*,†] André Colom,[*,†] Charlotte Guigné,[*,†] Laurens A. van Meeteren,[§] Wouter H. Moolenaar,[§] Philippe Valet,[*,†] and Jean Sébastien Saulnier-Blache[1,*,†]

Institut National de la Santé et de la Recherche Médicale (INSERM), U1048,* Toulouse, Cedex 4, France; Université de Toulouse, UPS, Institut de Médecine Moléculaire de Rangueil,† IFR150, BP84225, Toulouse, France; and Division of Cell Biology and Center for Biomedical Genetics,§ The Netherlands Cancer Institute, Amsterdam, The Netherlands

Abstract Autotaxin (ATX) is a secreted lysophospholipase D that generates the lipid mediator lysophosphatidic acid (LPA). ATX is secreted by adipose tissue and its expression is enhanced in obese/insulin-resistant individuals. Here, we analyzed the specific contribution of adipose-ATX to fat expansion associated with nutritional obesity and its consequences on plasma LPA levels. We established ATX$^{F/F}$/aP2-Cre (FATX-KO) transgenic mice carrying a null ATX allele specifically in adipose tissue. FATX-KO mice and their control littermates were fed either a normal or a high-fat diet (HFD) (45% fat) for 13 weeks. FATX-KO mice showed a strong decrease (up to 90%) in ATX expression in white and brown adipose tissue, but not in other ATX-expressing organs. This was associated with a 38% reduction in plasma LPA levels. When fed an HFD, FATX-KO mice showed a higher fat mass and a higher adipocyte size than control mice although food intake was unchanged. This was associated with increased expression of peroxisome proliferator-activated receptor (PPAR)γ2 and of PPAR-sensitive genes (aP2, adiponectin, leptin, glut-1) in subcutaneous white adipose tissue, as well as in an increased tolerance to glucose. These results show that adipose-ATX is a negative regulator of fat mass expansion in response to an HFD and contributes to plasma LPA levels.—Dusaulcy, R., C. Rancoule, S. Grès, E. Wanecq, A. Colom, C. Guigné, L. A. van Meeteren, W. H. Moolenaar, P.e Valet, and J. S. Saulnier-Blache. **Adipose-specific disruption of autotaxin enhances nutritional fattening and reduces plasma lysophosphatidic acid. *J. Lipid Res.* 2011.** 52: **1247–1255.**

Supplementary key words adipocyte • high-fat diet • obesity

Autotaxin (ATX) is a secreted lysophospholipase D that catalyzes the hydrolysis of lysophosphatidylcholine into lysophosphatidic acid (LPA), a growth factor-like lipid mediator acting via specific G-protein coupled receptors (1–3). ATX is present in plasma and other biological fluids and is expressed by several organs and tissues but the tissue origin of circulating LPA remains unknown. ATX plays a crucial role in embryonic development because its knockout in mice is lethal due to impaired blood vessel formation and a failure of neural tube closure (4–6).

So far, ATX has mostly been studied for its role in tumorigenesis, angiogenesis, and metastasis (7). Our group has brought ATX into the area of metabolic diseases. We have shown that ATX is abundantly expressed and secreted by adipocytes (8–10) and is responsible for the production of LPA in adipose tissue extracellular medium (11). Nevertheless, the specific contribution of adipose-ATX to circulating LPA remains unknown. ATX expression is increased in adipose tissue from obese/insulin-resistant mice and humans (9, 12). In vitro, ATX expression and secretion increase during the differentiation of preadipocytes into adipocytes (adipogenesis) (8, 9). These observations suggested that ATX contributes to fat development in obesity and associated pathologies. In the present study, we set out to disrupt ATX expression specifically in mouse adipose tissue to examine whether fat mass and plasma LPA concentration were affected. We demonstrate that adipocyte-specific disruption of ATX significantly increases the sensitivity of adipose tissue to expand in response to a high-fat diet (HFD) and directly influences plasma LPA levels.

This work was supported by grants from the INSERM, the Fondation pour la Recherche Médicale (grant # DRM20101220459), and the Dutch Cancer Society. R. Dusaulcy and C. Rancoule were supported by a grant from the Ministère de l'Education Nationale de la Recherche et de la Technologie (France).

Manuscript received 23 February 2011.

Published, JLR Papers in Press, March 18, 2011
DOI 10.1194/jlr.M014985

Abbreviations: ATX, autotaxin; FATX-KO, ATX$^{F/F}$/aP2-Cre; HFD, high-fat diet; LPA, lysophosphatidic acid; ND, normal diet; PPAR, peroxisome proliferator-activated receptor.

[1]To whom correspondence should be addressed.
e-mail: Jean-Sebastien.Saulnier-Blache@inserm.fr

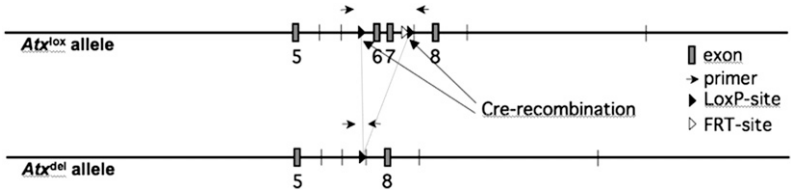

Fig. 1. Schematic representation of cre-mediated recombination of the floxed-ATX gene. Adapted from (4).

MATERIALS AND METHODS

Animals

Animals were handled in accordance with the principles and guidelines established by the National Institute of Medical Research (INSERM) and were in conformity with the Public Health Service Policy on Humane Care and Use of Laboratory Animals. The local Animal facility committee of INSERM approved our protocols. Mice were housed conventionally under a constant temperature (20–22°C) and humidity (50–60%) and with a 12/12 h light/dark cycle (lights on at 7:00 AM) and free access to food and water. The animals were fed either a normal diet (ND) [2900 kcal/kg: 16% protein, 81% carbohydrate, and 3% fat (SAFE, Augy, France)] or an HFD [4730 kcal/kg: 20% protein, 35% carbohydrate, and 45% fat (Research Diet, France)]. When the HFD was applied, it started at the age of 10 weeks for 13 weeks. Fat and lean mass was measured using dual-energy X-ray absorptiometry (EchoMRI-100TM, Echo Medical System, Houston, TX) in accordance with the manufacturer's instructions.

Establishment of $ATX^{F/F}$/aP2-Cre mice

$ATX^{F/F}$ (FVB genetic background) mice carrying a conditional *ATX* deleted allele in which exons 6 and 7 (encoding for the catalytic site of ATX) are flanked by two loxP sites were previously described (4). aP2-Cre mice (B6 genetic background) (Jackson Laboratory) carry a Cre transgene driven by promoter sequences from the fatty acid binding protein 4, a gene predominantly expressed in adipocytes (13). $ATX^{F/F}$ mice were mated to aP2-Cre mice and offspring were genotyped in order to select mice bearing both $ATX^{F/F}$ and aP2-Cre alleles (**Fig. 1**). $ATX^{F/F}$/aP2-Cre (FATX-KO) mice were compared with control $ATX^{F/F}$ littermates of the same generation.

Genotyping

Genotyping was performed by PCR on tail-tip DNA. The presence of the $ATX^{F/F}$ allele was determined by using the primers P583 (5′-TGCTTGAAGTGTGTGCAC-3′) and P584 (5′-TTGAATCCTGAGCAATATGG-3′) yielding 170 bp and 300 bp products for the wild-type and the floxed alleles, respectively (Fig. 1). Cycling conditions were: 34 cycles of 94°C for 30 s, 58°C for 30 s, and 72°C for 30 s.

The presence of the aP2-Cre allele was determined using the primers C001 (5′-ACCAGCCAGCTATCAACTCG-3′) and C002 (5′-TTACATTGGTCCAGCCACC-3′) yielding a 192 bp product. An internal PCR control targeting interleukin-2 gene was performed with primers C003 (5′-CTAGGCCACAGAATTGAAAGATCT-3′) and C004 (5′-GTAGGTGGAAATTCTAGCATCATCC-3′) yielding a 324 bp product. Cycling conditions were: 35 cycles of 94°C for 1 min, 60°C for 2 min, and 72°C for 1 min.

Adipose cell fractioning

Immediately after dissection, adipose tissue was minced and incubated for 30 min at 37°C under shaking in 5ml of Krebs-Ringer buffer supplemented with 1 mg/ml collagenase, 3.5 g/100 ml bovine serum albumin, and 22 mg /100 ml pyruvate. Digested tissue was filtered through a 150 μm screen and floating adipocytes were separated from infranatant, which was centrifuged at 900 *g* for 20 min in order to get stroma-vascular cells (preadipocytes, endothelial cells, and macrophages) in the pellet.

mRNA quantification

Total RNAs were extracted from tissues and cells using the RNeasy mini kit (Qiagen, GmbH, Hilden, Germany). Total RNA (500 ng) was reverse-transcribed for 60 min at 37°C using Superscript II reverse transcriptase (Invitrogen) in the presence of random hexamers. A minus RT reaction was performed in parallel

TABLE 1. Sequence of the oligonucleotide primer sets used in RT-PCR analysis

	Primer sequence 5′ to 3′	
Target genes	Sense	Antisense
ATX 6-7	TCCGTGCATCGTACATGAAGA	CAGGACCGCAGTTTCTCAATG
ATX 1-2	TGTTTCGGGTCATACCAGGTAAT	TCGACTTGCTGTGAATCCTAAGC
PPARγ2	CTGTTTTATGCTGTTATGGGTGAAA	GCACCATGCTCTGGGTCAA
FABP4 (aP2)	TTCGATGAAATCACCGCAGA	GGTCGACTTTCCATCCCACTT
CD11b	TCGGACGAGTTCCGGATTC	TGTGATCTTGGGCTAGGGTTTC
F4/80	TGACAACCAGACGGCTTGTG	GCAGGCGAGGAAAAGATAGTGT
CD31	GTCGTCCATGTCCCGAGAA	GCACAGGACTCTCGCAATCC
Adiponectin	TGGAATGACAGGAGCTGAAGG	TATAAGCGGCTTCTCCAGGCT
Leptin	GGGCTTCACCCCATTCTGA	TGGCTATCTGCAGCACATTTTG
Glut-1	GGTGTGCAGCAGCCTGTGT	CACAGTGAAGGCCGTGTTGA
Glut-4	CCGGATTCCATCCCACAAG	CATGCCACCCACAGAGAAGA
LPL	TTATCCCAATGGAGGCACTTTC	CACGTCTCCGAGTCCTCTCTCT
FAS	ATCCTGGAACGAGAACACGATCT	AGAGACGTGTCACTCCTGGACTT
UCP1	CCTGCCTCTCTCGGAAACAA	TGTAGGCTGCCCAATGAACA
CD45	ACATGCTGCCAATGGTTCTG	GTCCCACATGACTCCTTTCCTATG
PGC1α	AAAGGATGCGCTCTCGTTCA	GGAATATGGTGATCGGGAACA

ATX, autotaxin; PPAR, peroxisome proliferator activated receptor; FABP, fatty acid binding protein; CD, cluster of differentiation molecule; F4/80, EGF-like module containing, mucin-like, hormone receptor-like sequence 1; Glut, glucose transporter; LPL, lipoprotein lipase; FAS, fatty acid synthase; UCP, uncoupling protein; PGC, peroxisome proliferator-activated receptor γ, coactivator.

to ensure the absence of genomic DNA contamination. Real-time PCR was performed starting with 12.5 ng cDNA and 100 to 900 nM specific oligonucleotide primers in a final volume of 20 µl using the Mesa blue QPCR Master Mix for Sybr (Eurogentec). Fluorescence was monitored and analyzed in a StepOnePlus Real-Time PCR system instrument (Applied Biosystems). Analysis of the 18S rRNA was performed in parallel using the RRNA control Taqman Assay Kit (Applied Biosystem) in order to normalize gene expression levels. Results are expressed as follows: $2^{(Ct18S-Ctgene)}$ where Ct corresponds to the number of cycles needed to generate a fluorescent signal above a predefined threshold. Oligonucleotide primers were designed using the Primer Express software (Applied Biosystems). The sequence of the oligonucleotide primers is listed in **Table 1**.

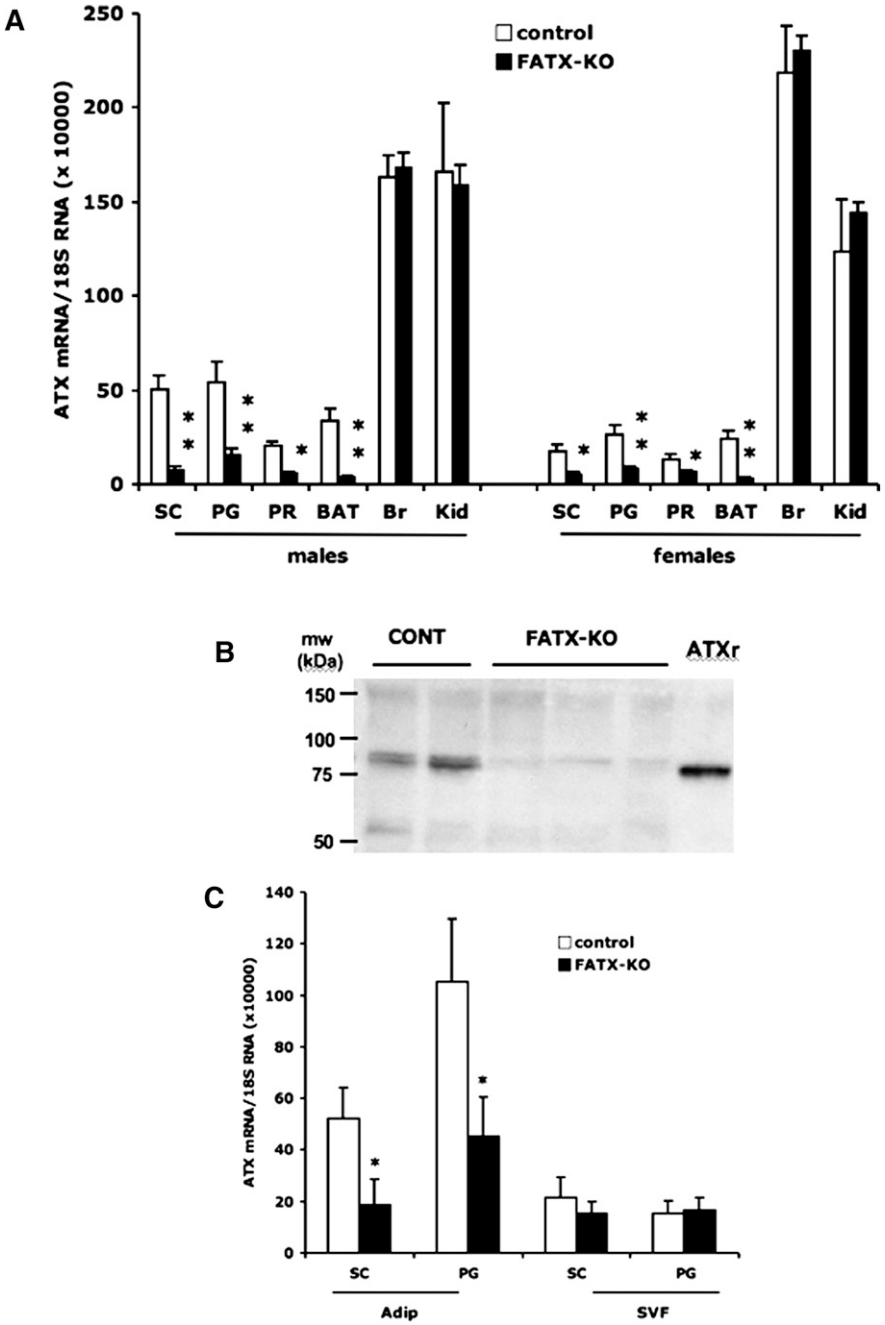

Fig. 2. Adipose-specific disruption of ATX. A: ATX mRNAs were quantified in subcutaneous (SC), perigonadal (PG), perirenal (PR) white adipose tissue, brown adipose tissue (BAT), brain, and kidney from control (8 males, 4 females) and FATX-KO (14 males, 17 females) mice fed a normal diet. Values are means ± SEM. B: ATX protein was detected by Western blot in subcutaneous white adipose tissue from 23 weeks old control (CONT, n = 2) and FATX-KO (n = 3) male mice. Recombinant mouse ATX (ATXr) expressed in Sf9-cells was used in parallel as a control. C: ATX mRNAs were quantified in the adipocyte (Adip) and the stroma-vascular (SVF) fractions isolated from the SC and PG white adipose tissue of control (n = 3) and FATX-KO (n = 4) male mice fed a normal diet. Values are means ± SEM. A Student's *t*-test was used to compare control with FATX-KO mice: * $P < 0.05$, ** $P < 0.01$.

Western blot analysis

Thirty micrograms of protein from concentrated conditioned medium were separated on a Gel CRITERION 4-12% (*Biorad*) and transferred on nitrocellulose membrane. The blot was preincubated for 1 h at room temperature in TBS/Tween 0.1% containing 5% dry milk and overnight at 4°C in the same solution supplemented with 0.7 μg/ml ATX-antibody. After washing in PBS/Tween 0.1%, ATX was visualized by enhanced chemioluminescence detection system (ECL, Amersham Biosciences) using an anti rabbit-HRP antibody (SIGMA). ATX-peptide (573-KNKLEELNKRLHT-KGS-588) antibody was purchased from Cayman Chemical.

Adipocyte cellularity measurement

Immediately after dissection, perigonadal and subcutaneous fat pads were fixed in ethanol 95% for 48 h, embedded in paraffin, and prepared on hematoxylin and eosin stained slides. Three nonoverlapping fields (300 to 1500 adipocytes) were captured with an analogic camera (Nikon DXM1200F) connected to a microscope (Nikon Eclipse TE2000-U). Adipocytes areas were measured with Lucia G software (Laboratory Imaging) and theoretical mean diameter was determined as $2\sqrt{}$ (area/pi). Adipocyte number per fat pad was determined as previously described (14) using the following formula: FPW $\times 10^6$ /[(4×Pi R^3/3)/1000]×0.95 with FPW (fat pad weight) in mg and R (radius) in μm.

Glucose tolerance test

Blood glucose concentrations were monitored with a glucose meter (Roche Diagnostic, Grenoble, France) at −30, 0, 30, 60, 90, and 120 min after gavage of fasting mice (6 h) with glucose (3 g/kg body weight).

Quantification of plasma LPA

LPA was quantified using a radioenzymatic assay as previously described (15). Briefly, lipids were extracted from conditioned media or plasma with an equal volume of 1-butanol and evaporated. Extracted lipids were converted into [^{14}C] PA with recombinant LPA acyl-transferase in the presence of [^{14}C] oleoyl-CoA. The products of the reaction were extracted, separated by one-dimensional TLC, and autoradiographed.

Statistics

Results are means ± SE. Student's *t*-test was used to compare two groups of data.

RESULTS

Adipose-specific disruption of ATX

ATX mRNAs were quantified using a set of oligonucleotide primers directed against exons 6 and 7, which are expected to be deleted after Cre-mediated recombination. When compared with their control littermates, FATX-KO mice exhibited a strong reduction (70 to 90% depending on fat depot) in ATX mRNA in perigonadal, subcutaneous, and perirenal white adipose tissue as well as in brown fat tissue (**Fig. 2A**). No significant change in ATX mRNA was observed in brain and kidney (Fig. 2A). Similar results were obtained in both males and females (Fig. 2A). Adipose-specific disruption of ATX mRNA was also observed when using another set of PCR primers directed against exons 1 and 2, which are out of the lox site framing (not shown), suggesting that cre-mediated recombination of exons 6 and 7 led to the complete loss of the whole ATX mRNA. This was confirmed using Western blot analysis that revealed a strong reduction in the amount of ATX protein in white adipose tissue of FATX-KO mice when compared with control mice (Fig. 2B). In white adipose tissue from control mice, ATX mRNA expression was higher in the adipocyte than in the stroma-vascular fraction (Fig. 2C). In FATX-KO mice, the disruption of ATX expression was observed in the adipocyte but not in the stroma-vascular fraction when compared with control mice (Fig. 2C). These results demonstrated that in FATX-KO mice possessed an adipocyte-specific disruption of ATX expression.

Adipose-specific disruption of ATX enhances white adipose tissue expansion in response to HFD

Under ND, FATX-KO mice (males and females) showed no significant change in body weight, adipose tissue (white and brown) mass, or in the weight of other organs (liver, kidney, heart, brain, and skeletal muscles) when compared with control mice (not shown). These results show that under ND, adipose-specific disruption of ATX does not affect the normal development of white and brown adipose tissue.

Under HFD, total body weight and the weight of other organs remained unchanged between control and FATX-KO males (**Table 2** and **Fig. 3A**). In females, a tendency of increase ($P = 0.076$) in total body weight was observed in FATX-KO when compared with control mice (Table 2). In parallel, a significantly higher weight of the three white adipose tissue depots as well as of brown adipose tissue was observed in FATX-KO when compared with control mice (Fig. 3A). This phenotype was particularly pronounced in females, (Fig. 3A). Analysis of body composition using

TABLE 2. Body weight and glycemia

			n	Body weight (g)	Plasma glucose (g/l)
Females	Normal diet	control	4	29.8 ± 2.5	0.85 ± 0.07
		FATX-KO	19	27.4 ± 1.9	1.03 ± 0.03
	High-fat diet	control	7	30.7 ± 2.4	1.14 ± 0.11
		FATX-KO	16	36.1 ± 2.9 (0.076)	1.27 ± 0.07
Males	Normal diet	control	8	32.3 ± 1.7	1.28 ± 0.16
		FATX-KO	14	34.2 ± 1.8	1.05 ± 0.07
	High-fat diet	control	6	45.2 ± 2.9	1.43 ± 0.13
		FATX-KO	15	47.6 ± 1.9	1.54 ± 0.13

Plasma glucose was determined after overnight fasting (*P*-value).

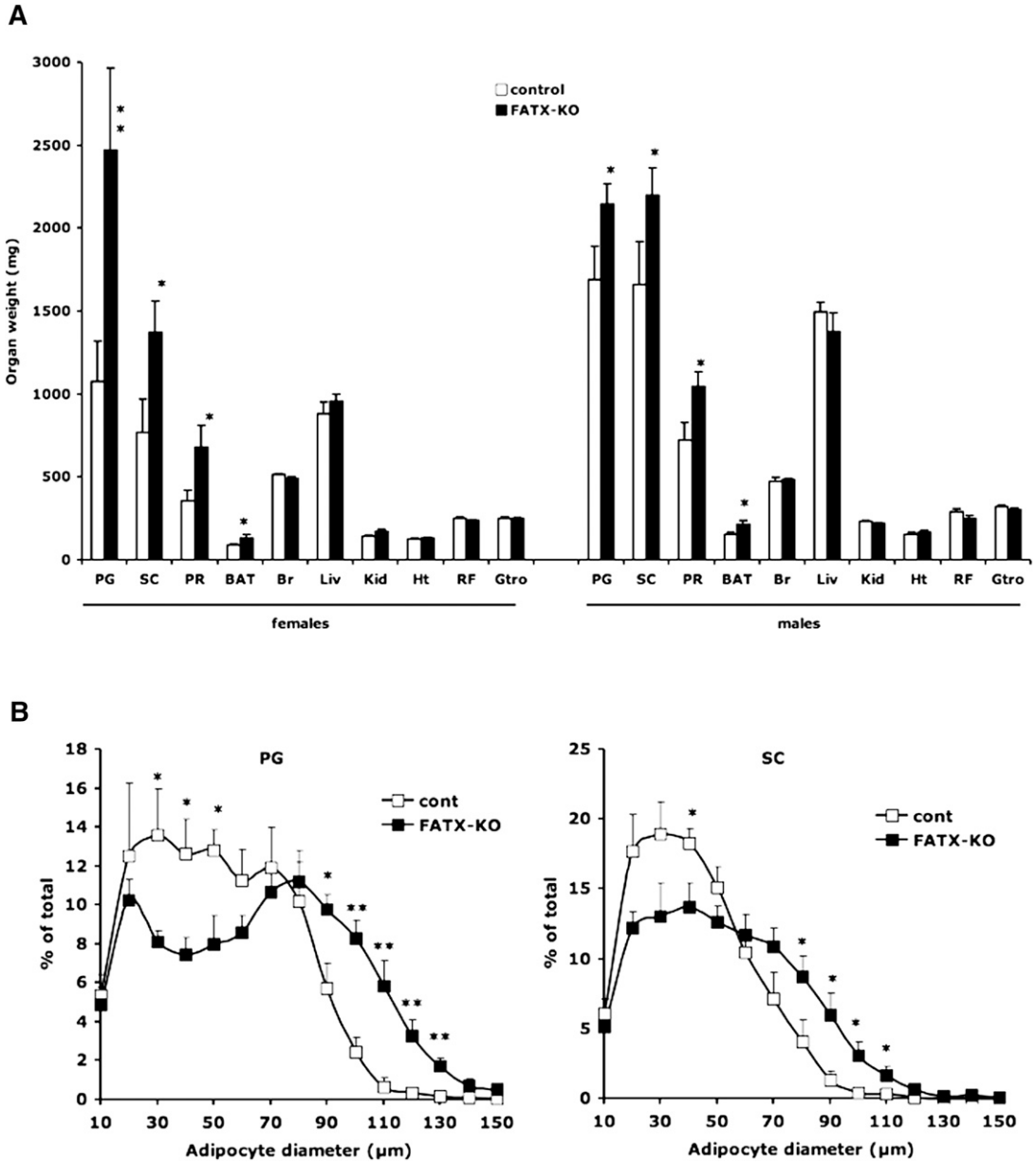

Fig. 3. Adipose-specific disruption of ATX enhances white adipose tissue mass in response to a high-fat diet (HFD). A: Control (white bars: 14 males and 19 females) and FATX-KO (black bars: 15 males and 19 females) mice were fed an HFD and their organs were weighed. PG, perigonadal adipose tissue; SC, subcutaneous adipose tissue; PR, perirenal adipose tissue; BAT, brown adipose tissue; Br, brain; Liv, liver; Kid, kidney; Ht, heart; RF, rectus femoris muscle; Gtro, gastrocnemus muscle. B: Adipocyte size distribution was analyzed in PG and SC from control (n = 5) and FATX-KO (n = 6) female mice fed an HFD. Values are means ± SEM. A Student's *t*-test was used for comparison: * $P < 0.05$, ** $P < 0.01$.

EchoMRI showed that on a HFD, FATX-KO females (n = 4) exhibited a significantly higher body fat mass than control females (n = 4) (42.1 ± 1.5 vs. 35.7 ± 2.1%, $P < 0.05$) with no significant change in body lean mass (47.0 ± 1.2 vs. 51.8 ± 2.1%). Adipocytes from female FATX-KO mice (n = 5) exhibited a higher mean size when compared with control mice (n = 6): 66 ± 6 versus 51 ± 4 µm in perigonadal fat ($P = 0.017$); 52 ± 3 versus 41 ± 3 µm in subcutaneous fat ($P = 0.039$). In parallel, no significant difference in adipocyte number (million per fat pad) was noticed between control and FATX-KO mice: 23 ± 5 versus 26 ± 3 for perigonadal adipose tissue; 23 ± 2 versus 24 ± 2 for subcutaneous adipose tissue. Analysis of adipocyte size distribution showed that FATX-KO mice exhibited a significantly higher proportion of the large adipocytes (higher than 80 and 70 µm in perigonadal and subcutaneous fat pads, respectively) associated with a lower proportion of small adipocytes (lower than 70 and 60 µm in perigonadal and subcutaneous fat pads, respectively) than control mice (Fig. 3B). These results show that adipose-specific disruption of ATX enhances the sensitivity of adipose tissue to expand in response to HFD as the consequence of an hypertrophy rather than an hyperplasia of the adipocytes.

The difference in adipose tissue expansion between control and FATX-KO mice fed an HFD was associated with no significant change in cumulative food intake: 9.5 ±

0.4 and 9.9 ± 0.4 g/week/g body weight for control (n = 8) and FATX-KO (n = 10) female mice, respectively. It thus appears that adipose-specific disruption of ATX has no influence on food intake, suggesting that a possible impact of ATX energy expenditure has to be considered in the future.

FATX-KO mice on an HFD showed no significant difference in fasting blood glucose when compared with control mice (Table 2). Nevertheless, the amplitude of the glycemic response curve obtained after an oral ingestion of glucose was attenuated in FATX-KO female when compared with control mice (**Fig. 4**). This attenuation was significant as attested by a the significant reduction of the area under the curve: 297 ± 23 versus 411 ± 34 arbitrary unit ($P = 0.012$) in FATX-KO and control mice, respectively. These results indicate the higher sensitivity of FATX-KO mice to expand fat mass, in response to HFD, is associated with a better glucose tolerance.

Adipose-specific disruption of ATX alters gene expression profile in subcutaneous white fat depot

To characterize the influence of ATX disruption on adipose tissue in further detail, we analyzed gene expression in white and brown adipose tissue. Because enhanced sensitivity of FATX-KOs to expand their white adipose tissue in response to an HFD was more pronounced in females than in males, we focused our analysis on females. The expression of peroxisome proliferator-activated receptor (PPAR)γ2, aP2, F4/80, adiponectin, leptin and Glut-1 genes was significantly higher in subcutaneous fat from FATX-KO than in control females. This was observed on both ND and HFD conditions (**Fig. 5A**, B). Immunohistomorphology of subcutaneous fat section revealed no detectable crown-like structure in either control and FATX-KO mice (not shown). In contrast to subcutaneous fat, no significant change in gene expression was observed in perigonadal adipose tissue between FATX-KO and control mice (Fig. 5 A and B). In brown adipose tissue, no significant change in gene expression was observed except for leptin, expression of which was higher in FATX-KO when compared with control mice in agreement with the higher brown adipose tissue mass (Fig. 3A). These results show that adipose tissue-specific disruption of ATX leads to a depot-specific alteration in gene expression profile, particularly in subcutaneous white adipose tissue.

White adipose tissue ATX contributes to plasma LPA

On an ND, FATX-KO mice showed a significant reduction (38%) in plasma LPA when compared with control mice (**Fig. 6A**). On an HFD, plasma LPA concentration was increased (62%) in control mice when compared with ND. In contrast, in FATX-KO mice, an HFD had no influence on plasma LPA concentration (Fig. 6A). HFD was associated with an increased expression of ATX mRNA in perigonadal and subcutaneous white adipose tissue of control mice, not in FATX-KO mice (Fig. 6B). Interestingly, the induction of ATX expression by an HFD was stronger in subcutaneous (3.5-fold) than in perigonadal (2.4-fold) fat depots. As a result, in control mice on an HFD, subcutaneous fat produced more (1.6-fold) LPA than by perigonadal fat (8.8 ± 1.2 vs. 5.2 ± 0.5 pmoles LPA/50 mg/6 h, n = 5; $P < 0.023$, paired *t*-test). HFD-mediated regulation of ATX was not observed in brown adipose tissue, brain, nor kidney (Fig. 6B). We concluded that white adipose tissue ATX expression significantly influences plasma LPA levels.

DISCUSSION

Our previous studies showed that some forms of obesity in mouse and human are associated with an upregulation of ATX that is mainly restricted to adipose tissue (9, 12). Therefore, the main objective of the present study was to determine the specific contribution of adipose tissue ATX in the development of obesity. To address this, we generated transgenic mice bearing an adipose-specific invalidation of ATX (FATX-KO mice) by using a tissue-specific Cre-lox approach, and we compared their ability to develop nutritional obesity with control littermates. The chosen Cre-lox strategy was based on the predominant cre-recombinase activity in adipose tissue driven by the aP2-promoter (16). Our strategy was successful because a potent disruption of ATX was obtained in white and brown adipose tissue but not in other ATX-expressing organs. In addition, we observed that, in white adipose tissue from FATX-KO mice, the disruption of ATX was restricted to adipocytes and was not observed in the stroma-vascular fraction that also expresses ATX. This is in agreement with the predominant driving activity of the aP2-promoter in

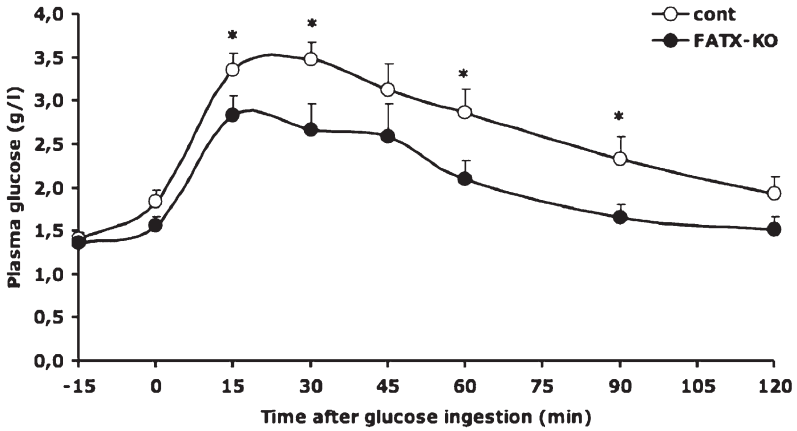

Fig. 4. Adipose-specific disruption of ATX improves glucose tolerance. Control (n = 8) and FATX-KO (n = 7) female mice were fed an HFD. Plasma glucose concentration was determined before and at different time points after an oral ingestion of a single dose of glucose. Areas under the curve were 411 ± 34 versus 297 ± 23 arbitrary unit ($P = 0.012$) in control and FATX-KO mice, respectively. A Student's *t*-test was used for comparison: * $P < 0.05$.

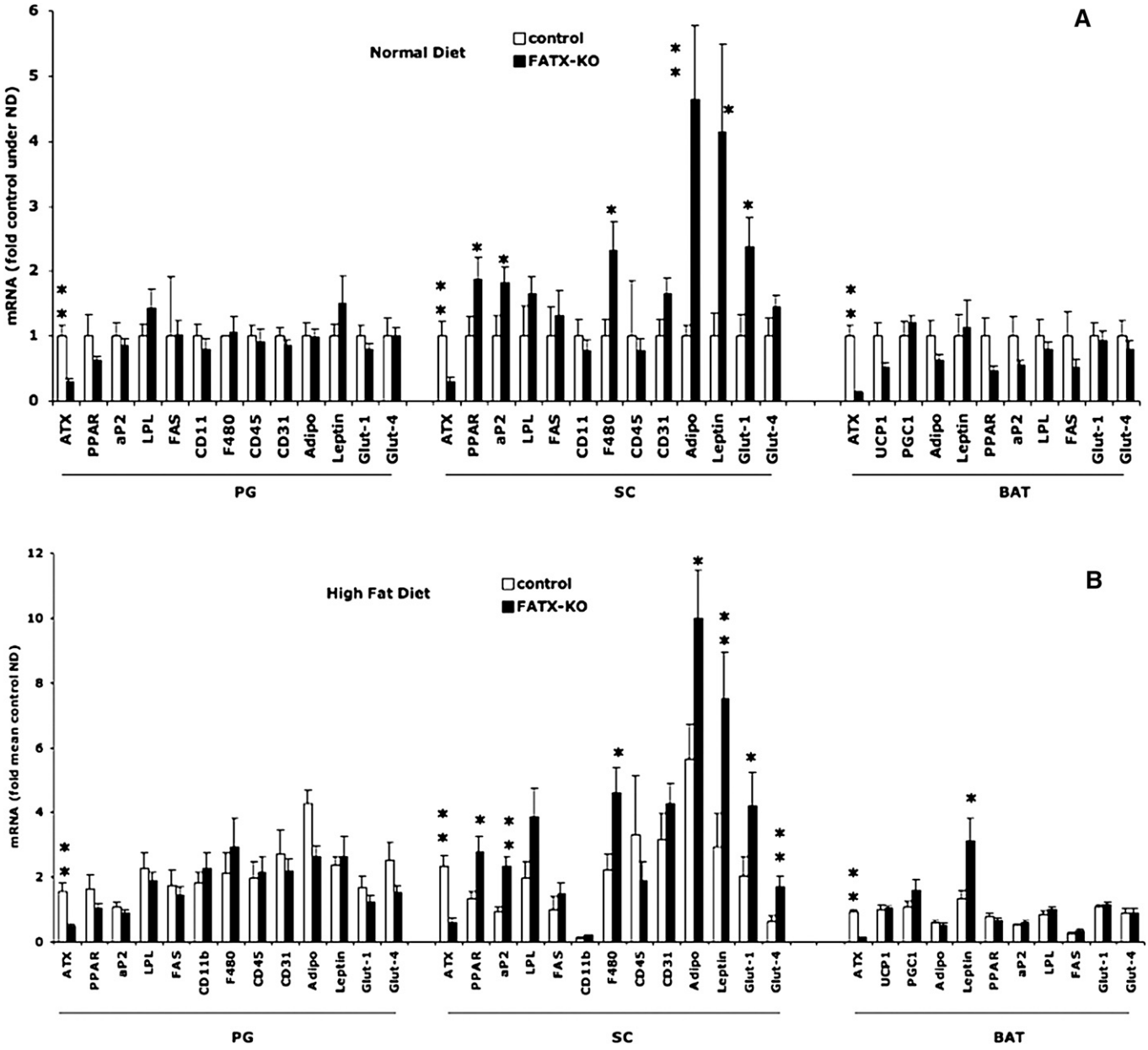

Fig. 5. Adipose-specific disruption of ATX alters gene expression in subcutaneous adipose tissue. Control and FATX-KO mice were fed either a normal diet (ND) (A) or a high-fat diet (HFD) (B) and gene expression was analyzed by real time PCR in perigonadal (PG), subcutaneous (SC), and brown adipose tissue (BAT). Values are means ± SEM from n mice (4 ND and 8 HFD for control; 14 ND and 15 HFD for FATX-KO). A Student's *t*-test was used for comparison: * $P < 0.05$, ** $P < 0.01$. ATX, autotaxin; PPAR, peroxisome proliferator-activated receptor; FABP, fatty acid binding protein; CD, cluster of differentiation molecule; F4/80, EGF-like module containing, mucin-like, hormone receptor-like sequence 1; Glut, glucose transporter; LPL, lipoprotein lipase; FAS, fatty acid synthase; UCP, uncoupling protein; PGC, peroxisome proliferator-activated receptor γ, coactivator.

adipocytes (17), and shows that FATX-KO mice bear an adipocyte-specific disruption of ATX.

Our main finding was that, when fed an HFD, FATX-KO mice exhibited a significantly higher fat mass than control mice. This shows that adipose-specific disruption of ATX increases the sensitivity of adipose tissue to expand when exposed to an HFD, strongly suggesting that adipose tissue-ATX participates in a negative feedback regulation of nutritional obesity. Interestingly, this negative feedback of ATX was not evidenced in mice fed an ND. One can hypothesize that a threshold of ATX expression needs to be reached to get a negative regulation of fat mass. Thus, ATX expression in control mice is likely too low to exert its inhibitory action so that its disruption in FATX-KO mice has no significant impact on fat mass. In contrast, on an HFD, the expression of ATX is increased above the critical threshold, leading to a significant inhibitory effect on fat mass which, when suppressed in FATX-KO mice, leads to a higher fat mass than in control mice.

The expansion of fat mass in response to HFD is known to result from an increased storage capacity of adipocytes

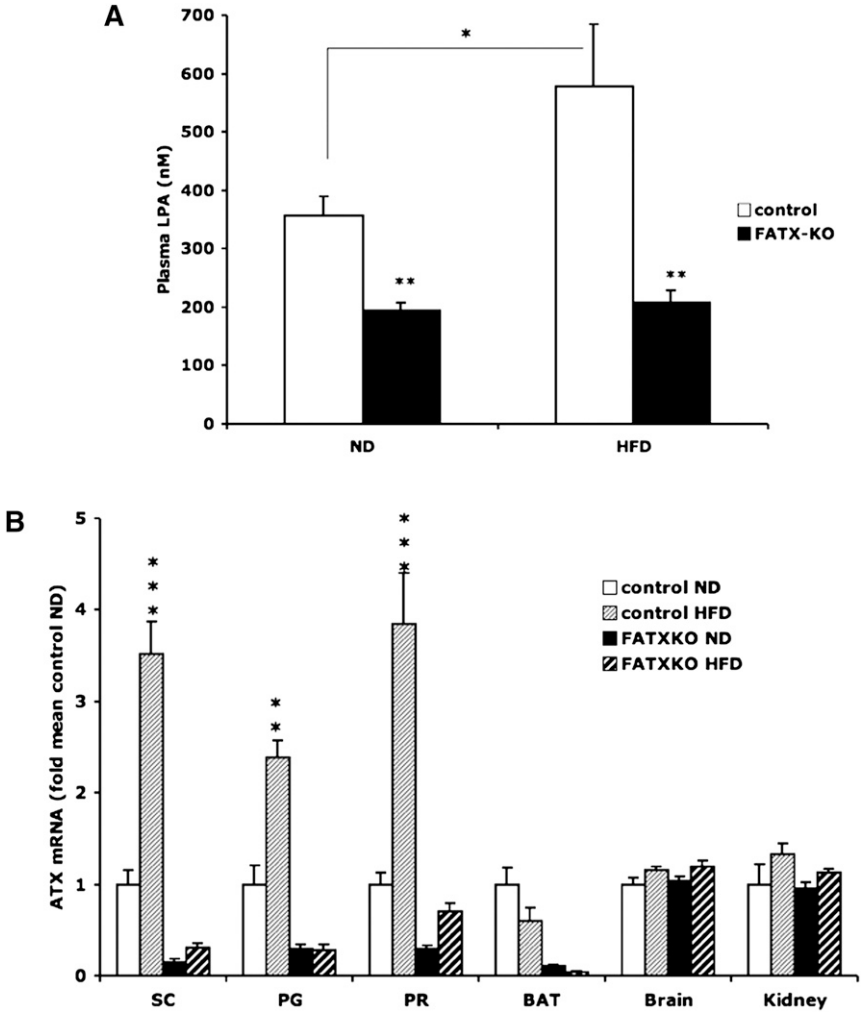

Fig. 6. Adipose-ATX contributes to plasma LPA. Plasma LPA concentration (A) and the expression of ATX gene in perigonadal (PG), subcutaneous (SC), perirenal (PR), brown adipose tissue (BAT), brain, and kidney (B) were quantified in control and FATX-KO male mice fed either a normal diet (ND) or a high-fat diet (HFD). Values are means ± SEM from 4 control ND, 6 control HFD, 14 FATX-KO ND, and 15 FATX-KO HFD mice. A Student's *t*-test was used for comparison: * $P < 0.05$, ** $P < 0.01$, *** $P < 0.001$.

combined with the recruitment of new adipocytes by differentiation of dormant preadipocytes, a process termed adipogenesis. We previously demonstrated that LPA, the product of ATX activity, has an anti-adipogenic activity that was associated with downregulation of PPARγ2, a master transcription factor involved in adipocyte differentiation (18). We propose that the hypersensitivity of FATX-KO mice to expand fat mass in response to an HFD might result, at least in part, from the alleviation of the anti-adipogenic effect of LPA produced by adipose tissue. This hypothesis is supported by our findings that subcutaneous adipose tissue from FATX-KO mice exhibits an increased expression of PPARγ2 and several PPARγ2-regulated genes such as aP2, adiponectin, leptin, glut-1, and glut-4 (19, 20). It is unclear why this increase was observed in subcutaneous adipose tissue but not in other fat depots. One possible explanation is that in control mice, the induction by an HFD of ATX expression and LPA production are more pronounced in subcutaneous than in perigonadal. Therefore, the inhibitory action of ATX on gene expression is expected to be more pronounced in subcutaneous than in perigonadal fat. Consequently, gene upregulation associated with ATX disruption is expected to be more pronounced in subcutaneous than in perigonadal fat. Another possibility is that, in other depots, ATX acts via a different mechanism. Indeed, it was shown that in contrast to subcutaneous fat, visceral fat expansion in response to an HFD does not involve adipogenesis but rather involves an increased storage capacity of existing adipocytes (21). Besides its involvement in adipogenesis, PPARγ2 is also known to increase the storage capacity of adipocytes by improving glucose uptake (22). Consequently, in parallel with its anti-adipogenic impact, ATX could also negatively regulate the storage capacity of adipocytes, for example, by inhibiting glucose homeostasis. This hypothesis is supported by our data showing that FATX-KO mice have larger adipocytes and a better glucose tolerance than control mice.

Finally, the present study also provides insight into the contribution of adipose-ATX to plasma LPA levels. ATX is

the main source of plasma LPA (4). Various organs express ATX, including adipose tissue, but their respective contribution to plasma LPA has been elusive. We observed that plasma LPA is significantly reduced in FATX-KO mice when compared with control mice. Conversely, plasma LPA increases when control mice are fed an HFD and this is accompanied by an upregulation of ATX, specifically in white adipose tissue. These observations clearly indicate that up- or down-regulating ATX in white adipose tissue correlates with plasma LPA concentration. Therefore, we conclude that adipose tissue significantly contributes to plasma LPA. In addition, these results show that the mechanisms by which adipose-ATX regulate fat expansion in response to an HFD could result from a combination of a local and endocrine production of LPA by the adipose tissue.

In conclusion, the present study demonstrates that adipose-ATX negatively regulates fat mass expansion in response to an HFD and contributes to plasma LPA levels. Although the mechanism by which it affects the physiology of adipose tissue in mice remains to be clarified, the present work strongly demonstrates the involvement of adipose-ATX in the development of nutritional obesity.

The authors thank Yara Barreira and Myriam Ben-Neji (IFR150, Animal Facility) and Sophie Legonidecq and Aurore Desquesnes (IFR150, Functional Exploration Service) for their technological assistance.

REFERENCES

1. van Meeteren, L. A., and W. H. Moolenaar. 2007. Regulation and biological activities of the autotaxin-LPA axis. *Prog. Lipid Res.* **46:** 145–160.
2. Yuelling, L. M., and B. Fuss. 2008. Autotaxin (ATX): a multi-functional and multi-modular protein possessing enzymatic lysoPLD activity and matricellular properties. *Biochim. Biophys. Acta.* **1781:** 525–530.
3. Boutin, J. A., and G. Ferry. 2009. Autotaxin. *Cell. Mol. Life Sci.* **66:** 3009–3021.
4. van Meeteren, L. A., P. Ruurs, C. Stortelers, P. Bouwman, M. A. van Rooijen, J. P. Pradere, T. R. Pettit, M. J. Wakelam, J. S. Saulnier-Blache, C. L. Mummery, et al. 2006. Autotaxin, a secreted lysophospholipase D, is essential for blood vessel formation during development. *Mol. Cell. Biol.* **26:** 5015–5022.
5. Tanaka, M., S. Okudaira, Y. Kishi, R. Ohkawa, S. Iseki, M. Ota, S. Noji, Y. Yatomi, J. Aoki, and H. Arai. 2006. Autotaxin stabilizes blood vessels and is required for embryonic vasculature by producing lysophosphatidic acid. *J. Biol. Chem.* **281:** 25822–25830.
6. Fotopoulou, S., N. Oikonomou, E. Grigorieva, I. Nikitopoulou, T. Paparountas, A. Thanassopoulou, Z. Zhao, Y. Xu, D. L. Kontoyiannis, E. Remboutsika, et al. 2010. ATX expression and LPA signalling are vital for the development of the nervous system. *Dev. Biol.* **339:** 451–464.
7. Liu, S., M. Murph, N. Panupinthu, and G. B. Mills. 2009. ATX-LPA receptor axis in inflammation and cancer. *Cell Cycle.* **8:** 3695–3701.
8. Gesta, S., M. F. Simon, A. Rey, D. Sibrac, A. Girard, M. Lafontan, P. Valet, and J. S. Saulnier-Blache. 2002. Secretion of a lysophospholipase D activity by adipocytes: involvement in lysophosphatidic acid synthesis. *J. Lipid Res.* **43:** 904–910.
9. Ferry, G., E. Tellier, A. Try, S. Gres, I. Naime, M. F. Simon, M. Rodriguez, J. Boucher, I. Tack, S. Gesta, et al. 2003. Autotaxin is released from adipocytes, catalyzes lysophosphatidic acid synthesis, and activates preadipocyte proliferation. Up-regulated expression with adipocyte differentiation and obesity. *J. Biol. Chem.* **278:** 18162–18169.
10. Pradere, J. P., E. Tarnus, S. Gres, P. Valet, and J. S. Saulnier-Blache. 2007. Secretion and lysophospholipase D activity of autotaxin by adipocytes are controlled by N-glycosylation and signal peptidase. *Biochim. Biophys. Acta.* **1771:** 93–102.
11. Ferry, G., N. Moulharat, J. P. Pradere, P. Desos, A. Try, A. Genton, A. Giganti, M. Beucher-Gaudin, M. Lonchampt, M. Bertrand, et al. 2008. S32826, a nanomolar inhibitor of autotaxin: discovery, synthesis and applications as a pharmacological tool. *J. Pharmacol. Exp. Ther.* **327:** 809–819.
12. Boucher, J., D. Quilliot, J. P. Praderes, M. F. Simon, S. Gres, C. Guigne, D. Prevot, G. Ferry, J. A. Boutin, C. Carpene, et al. 2005. Potential involvement of adipocyte insulin resistance in obesity-associated up-regulation of adipocyte lysophospholipase D/autotaxin expression. *Diabetologia.* **48:** 569–577.
13. He, W., Y. Barak, A. Hevener, P. Olson, D. Liao, J. Le, M. Nelson, E. Ong, J. M. Olefsky, and R. M. Evans. 2003. Adipose-specific peroxisome proliferator-activated receptor gamma knockout causes insulin resistance in fat and liver but not in muscle. *Proc. Natl. Acad. Sci. USA.* **100:** 15712–15717.
14. Morin, C. L., E. C. Gayles, D. A. Podolin, Y. Wei, M. Xu, and M. J. Pagliassotti. 1998. Adipose tissue-derived tumor necrosis factor activity correlates with fat cell size but not insulin action in aging rats. *Endocrinology.* **139:** 4998–5005.
15. Saulnier-Blache, J. S., A. Girard, M. F. Simon, M. Lafontan, and P. Valet. 2000. A simple and highly sensitive radioenzymatic assay for lysophosphatidic acid quantification. *J. Lipid Res.* **41:** 1947–1951.
16. Barlow, C., M. Schroeder, J. Lekstrom-Himes, H. Kylefjord, C. X. Deng, A. Wynshaw-Boris, B. M. Spiegelman, and K. G. Xanthopoulos. 1997. Targeted expression of Cre recombinase to adipose tissue of transgenic mice directs adipose-specific excision of loxP-flanked gene segments. *Nucleic Acids Res.* **25:** 2543–2545.
17. Graves, R. A., P. Tontonoz, S. R. Ross, and B. M. Spiegelman. 1991. Identification of a potent adipocyte-specific enhancer: involvement of an NF-1-like factor. *Genes Dev.* **5:** 428–437.
18. Simon, M. F., D. Daviaud, J. P. Pradere, S. Gres, C. Guigne, M. Wabitsch, J. Chun, P. Valet, and J. S. Saulnier-Blache. 2005. Lysophosphatidic acid inhibits adipocyte differentiation via lysophosphatidic acid 1 receptor-dependent down-regulation of peroxisome proliferator-activated receptor gamma2. *J. Biol. Chem.* **280:** 14656–14662.
19. Iwaki, M., M. Matsuda, N. Maeda, T. Funahashi, Y. Matsuzawa, M. Makishima, and I. Shimomura. 2003. Induction of adiponectin, a fat-derived antidiabetic and antiatherogenic factor, by nuclear receptors. *Diabetes.* **52:** 1655–1663.
20. Nugent, C., J. B. Prins, J. P. Whitehead, D. Savage, J. M. Wentworth, V. K. Chatterjee, and S. O'Rahilly. 2001. Potentiation of glucose uptake in 3T3–L1 adipocytes by PPAR gamma agonists is maintained in cells expressing a PPAR gamma dominant-negative mutant: evidence for selectivity in the downstream responses to PPAR gamma activation. *Mol. Endocrinol.* **15:** 1729–1738.
21. Joe, A. W., L. Yi, Y. Even, A. W. Vogl, and F. M. Rossi. 2009. Depot-specific differences in adipogenic progenitor abundance and proliferative response to high-fat diet. *Stem Cells.* **27:** 2563–2570.
22. Takano, H., and I. Komuro. 2009. Peroxisome proliferator-activated receptor gamma and cardiovascular diseases. *Circ. J.* **73:** 214–220.